J. Phys. C: Solid State Phys., Vol. 12, 1979. Printed in Great Britain. © 1979

Quadrupole splitting of Mössbauer lines due to defects in CoO

Nuria Barberan†, P W Tasker and A M Stoneham
Theoretical Physics Division, AERE, Harwell, Oxfordshire OX11 0RA, UK

Received 23 February 1979

Abstract. The Fe^{3+} lines observed in CoO Mössbauer sources may arise from the decay of Co^{3+} ions associated with cation vacancies in the crystal. These defects produce an electric-field gradient that causes a quadrupole splitting of the resonance line and that can, in principle, distinguish between different types of defects. The calculation of the quadrupole splitting at Fe^{2+} and Fe^{3+} sites near various vacancy clusters includes the relaxation of the lattice about the defect. This lattice polarisation and distortion is shown to be extremely important, since simple calculations based on perfect ion positions give very different field gradients at neighbouring sites. The results are compared with the experiments available and the quadrupole splittings observed are close to those predicted by a vacancy model.

1. Introduction

One of the problems that has concerned physicists working with the Mössbauer effect is the necessity for strong, single-line sources with which several types of target can be investigated. A particularly interesting case is ^{57}CoO (Ok and Mullen 1968) used for studying targets containing iron compounds. This material has several advantages over the commonly used ^{57}Co-doped sources, since it has a large recoil-free fraction at room temperature. Materials containing Co make very strong sources and a CoO source can avoid line broadening in doped materials because of interactions with neighbouring impurities. However, it is well known (see e.g. Wertheim, 1961) that several different cation charge states are observed in these oxide sources. In particular, the Mössbauer spectrum obtained using CoO as a source or target shows peaks due to Fe^{2+} and Fe^{3+} or even higher charge states (Ingalls and DePascuali 1965), the proportions of which depend on the method of preparation (Sond and Mullen 1976). The literature reports many experimental attempts to develop a standard method of making a single-line CoO source, but this has not yet been achieved.

The origin of the ferric ions in CoO sources is controversial and several interpretations of the observation exist. It has been suggested (Ingalls and De Pascuali 1965) that metastable charge states of iron are produced by an Auger process following the electron-capture disintegration of ^{57}Co. Alternatively the coexistence of several types of stoichiometric oxide (Mullen and Ok 1966) or microcrystalline CoO with cation defects (Schroeer and Triftshäuser 1968) has been proposed. The most common interpretation (Leon and Negrete 1970, Triftshäuser and Craig 1966, Tejada and Fontcuberta 1978) is the stabilisation of highly charged cation states by neighbouring vacancies. Catlow *et al* (1977a) have calculated the probable defect structure of CoO and shown

† Permanent address: Facultad de Ciencias, Universidad de Barcelona, Barcelona, Spain.

0022-3719/79/183827 + 09 $01.00

that complicated vacancy–hole (i.e. trivalent cation) complexes are likely. We have, therefore, calculated the quadrupole interaction on the nucleus of the emitting ion for each of the probable vacancy clusters. The values obtained for the quadrupolar splitting in Fe^{3+} or Fe^{2+} can, in principle, determine the defect structure of the crystal and will show whether the presence of Fe^{3+} in CoO sources can be due to the cation vacancies. Our calculations will also assess the importance of including correct lattice relaxation about a defect structure, rather than determining quadrupole splittings from the ideal lattice geometry. The quadrupole interaction is determined from the electric-field gradient at the iron sites and is evaluated after the lattice has been relaxed to equilibrium. The methods used here have a general application to the calculation of such interactions in nuclear research and spectroscopy.

2. The calculation

2.1. Vacancy clusters

Catlow *et al* (1977a) have calculated the vacancy–hole binding energies for various vacancy clusters in the divalent metal oxides. They used the same lattice-relaxation methods as used here to allow the ions to relax around the defect. The main conclusion was that it is inadequate to consider defects in these oxides without allowing for vacancy aggregation, and that simple single-vacancy–hole pairs will only dominate the defect structure in the stoichiometric case. Larger vacancy clusters are important for deviations greater than 10^{-3} from the stoichiometric composition. Even in more stoichiometric materials Schroeer and Triftshäuser (1968) have suggested that non-stoichiometric microcrystals may exist with the excess oxygens incorporated at the grain boundary.

These calculations consider explicitly both a simple single-vacancy structure and the most probable vacancy aggregate consisting of four vacancies and one interstitial

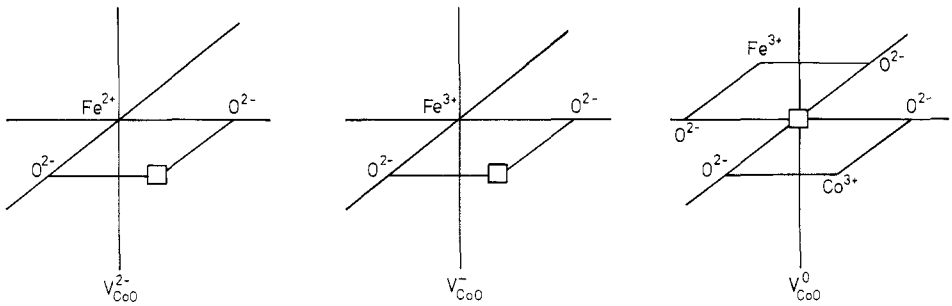

Figure 1. The three types of single-vacancy defects used for the calculation of electric-field gradients at Fe impurities in a CoO lattice.

in a cluster. The electric-field gradient has been calculated at an iron site in CoO for three distinct defects associated with a single vacancy. These are shown in figure 1 as the V^0, V^- and V^{2-} centres. In the first case the charge is neutral since two holes are bound to the vacancy on adjacent cation sites. One of these sites gives rise to an Fe^{3+} on decay whose γ emission is observed by the Mössbauer technique. Similarly the V^- centre has one bound hole on an Fe^{3+} ion, and the V^{2-} centre has no associated hole and so produces, on decay, an Fe^{2+} ion. Fe^{2+} ions will, of course, also exist in the bulk

of the crystal but there the lattice makes no contribution to the quadrupole splitting. Electrical neutrality is achieved by isolated hole centres elsewhere in the lattice which do not contribute significantly to the electric-field gradient at the defect centre.

The 4:1 vacancy cluster is the basic defect aggregate considered by Catlow *et al* (1977c) in the metal oxides. In highly non-stoichiometric materials these clusters may

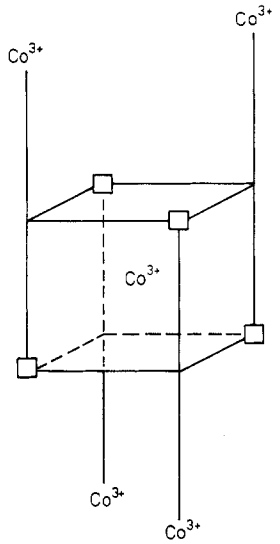

Figure 2. 4:1 cluster in the CoO lattice with Co^{3+} ions in octahedral positions and tetrahedral interstitial site explicitly shown.

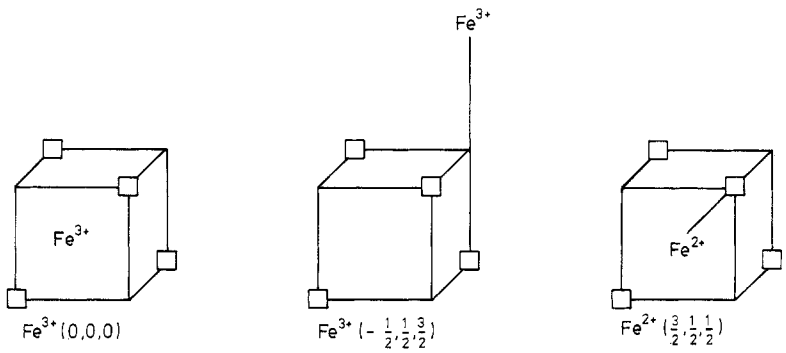

Figure 3. Fe impurity sites associated with the 4:1 cluster. Additional $Co^{3\bullet}$ ions are present as indicated in figure 2.

themselves aggregate to produce extended defects and new phases. However, only the basic cluster will be considered here. This defect consists of four cation vacancies placed in the vertices of a cube and one interstitial Co^{3+} in the centre of the cube in tetrahedral symmetry. A neutral cluster can be obtained by substituting five more Co^{3+} ions on cation sites and we have included four of them in positions of high symmetry. The additional hole is assumed, as before, not to be bound closely to the centre and hence does not contribute to the field gradient. The structure of this cluster is shown in

figure 2. Fe^{3+} ions are produced by the decay of Co^{3+} ions at either the interstitial site at the centre of the cube or at one of the octahedral substitutional sites and Fe^{2+} ions are created at normal associated Co^{2+} octahedral sites. These three possibilities are illustrated in figure 3.

In the experimental preparation of CoO sources a spinel phase is known to be present in the resulting material. Consequently we have also calculated the quadrupole splitting for Fe^{2+} and Fe^{3+} in the appropriate spinel material in order to distinguish between this phase and defect structures in normal CoO. The vacancy clusters considered here are a representative rather than exhaustive set and should enable the magnitude of the lattice contribution to the electric-field gradient to be calculated.

2.2. *Lattice relaxations*

An ionic model of CoO has been used in all these calculations with short-range potentials parameterised from the bulk properties. The ions are relaxed to equilibrium about the defect using the HADES program. This program considers a region of crystal around the defect in which all the atoms are explicitly treated and an outer region treated as a continuum and matched using the Mott–Littleton method (Mott and Littleton 1938). Details of the method have been given elsewhere (Norgett 1974, Lidiard and Norgett 1972) and the method has been used in many other studies of defects in ionic crystals (see e.g. Norgett *et al* 1977, Catlow *et al*, 1977b). The program calculates exactly all the Coulomb sums and the additional short-range interionic potentials are taken from the work of Catlow *et al* (1977b). The cation–anion and anion–anion potentials take the form

$$V_{+-}(r) = A_{+-}\exp(-r/\rho_{+-}) \qquad V_{--}(r) = A_{--}\exp(-r/\rho_{--}) - C_{--}/r^6 \tag{1}$$

where the parameters A, ρ and C are given in table 1. There is no short-range interaction

Table 1. Short-range potentials of the form $V(r) = A\exp(-r/\rho) - Cr^{-6}$ used in the calculations. Only the oxygen atom is polarisable with shell-model parameters as given.

Interaction	A (eV)	ρ (Å)	C(eV Å^{-6})
O^{2-}–O^{2-}	22764·3	0·1490	20·37
Co^{2+}–O^{2-}	793·2	0·3296	0·0
Fe^{2+}–O^{2-}	745·33	0·3362	0·0
Fe^{3+}–O^{2-}	702·29	0·3362	0·0
Lattice constant a = 4·26 Å			
Oxygen shell charge = $-2{\cdot}0066\lvert e\rvert$			
Spring constant = 4·81 eV Å^{-2}.			

between the cations. The polarisation of the ions is included by the shell model (Dick and Overhäuser 1958) in which each ion is considered as a core and shell coupled by an harmonic potential. The parameters are given in table 1 and reproduce well the dielectric properties of the crystal.

2.3. *Quadrupole splitting*

The excited nuclear state of Fe has a total spin of $I = \frac{3}{2}$ and the ground state has $I = \frac{1}{2}$.

Thus in a polycrystalline material, where the emission has no angular dependence, the energy splitting of the Mössbauer line is given by

$$\Delta E = \tfrac{1}{2}eQq(1 - \tfrac{1}{3}\eta^2)^{1/2} \tag{2}$$

where e is the electron charge, Q the quadrupole moment of the nucleus and q and η are derived from components of the electric-field gradient at the nucleus. The electric-field gradient has a contribution from the asymmetric distribution of charge due to the surrounding ions in the lattice and from the non-cubic distribution of electrons in partially filled orbitals on the atom itself. The lattice contribution is

$$V_{\alpha\beta} = \sum_{\text{ions, } K} Z^K/(r^K)^3[\delta_{\alpha\beta} - (3r_\alpha^K r_\beta^K)/(r^K)^2] \tag{3}$$

where $V_{\alpha\beta}$ is an element of the electric-field gradient tensor. The sum is over all ions K in the lattice of charge Z^K and distance r^K from the Mössbauer nucleus; r_α^K is the α component of the vector $\boldsymbol{r}^K$. The resulting tensor has zero trace and in the principal axis representation is diagonal with components named according to the convention

$$|V_{zz}| \geqslant |V_{yy}| \geqslant |V_{xx}|. \tag{4}$$

The asymmetry parameter η is given by

$$\eta = (V_{xx} - V_{yy})/V_{zz}. \tag{5}$$

The V_{zz} component of the field gradient at the nucleus is enhanced by the electron distortion of the Mössbauer atom and is modified by the Sternheimer antishielding factor γ_∞. Thus q in equation (2) is given by

$$q = (1 - \gamma_\infty)V_{zz} + (1 - R)\tfrac{4}{7}\langle r^{-3}\rangle_{3d} \tag{6}$$

where the second term is the electronic contribution to the field gradient modified by a

Table 2. Parameters used in the calculation of the energy splitting. Nuclear quadrupole moment, Q from Sharma (1971); $(1 - \gamma_\infty)$ from Sen and Narasimhan (1976); $(1 - R)$ from Ingalls (1964) and $\langle r^{-3}\rangle_{3d}$ from Freeman and Watson (1965).

Q	$= 0{\cdot}18 \times 10^{-24}$ cm^2
$(1 - \gamma_\infty)$	$= 10{\cdot}64$
$(1 - R)$	$= 0{\cdot}68$
$\langle r^{-3}\rangle_{3d}$	$= 5{\cdot}0809$ au (Fe^{2+})

Sternheimer shielding factor R. The values for the parameters used in these calculations are given in table 2. The Fe^{3+} and Fe^{2+} ions are in high-spin states and so the Fe^{3+} ground state has ^6S symmetry. There will be no contribution to the field gradient from this spherically symmetrical state and observation of this ion provides a sensitive test of the lattice field gradient. The electronic contribution, however, is large for Fe^{2+} (^5D) and will be shown to dominate the lattice term.

The lattice sum in equation (3) is carried out explicitly over the relaxed ionic coordinates (cores and shells) generated in the defect calculation. Convergence of the value to within a few per cent is achieved with a spherical lattice region of approximately 7·0 interionic distances. If the field gradient is obtained as a function of radius of region included in the sum, the values do not decrease monotonically, but oscillate as each

Table 3. Values of $(a^3/e)V_{zz}$ in a tetragonal distorted lattice; $a = b \neq c$, $\alpha = c/a$ with singly charged ions.

Radius in units of interionic distance	$\alpha = 0{\cdot}8$	$\alpha = 1{\cdot}26$	$\alpha = 1{\cdot}7$
5·0	6·949	4·582	7·977
6·0	6·721	4·607	7·655
7·0	6·736	4·473	7·866
8·0	6·772	4·522	7·690
∞†	6·725	4·575	7·753

† Values taken from summation given by De Wette 1961

successive shell of ions is included. These oscillations decrease as the sum converges. The results in table 4 are obtained by extrapolating the envelope of the curve to achieve greater accuracy. The resulting tensor is diagonalised to obtain the principle components of the field gradient. The approach can be checked against previous work. De Wette (1961) has calculated field gradients for tetragonal lattices, which is equivalent to distorting a cubic lattice along one axis. He used a method of summing over planes, whereas we have used an explicit summation over a sphere of ions, since we are considering point defects. Table 3 provides a comparison between his results and those obtained by summing over the sphere. It can be seen that they agree to within a few per cent.

3. Results and discussion

The defect clusters employed in these calculations have been described in § 2.1, and the hole that is bound to the vacancies is considered as trapped on an adjacent cation. This hole can hop to equivalent sites around the vacancies with a rate that depends on the overlap of the wavefunction on neighbouring ions. In the case of the V^0 centre (figure 1) this would lead to altered field gradients at the Fe^{3+} site. Similarly in the case of the 4:1 cluster, the hole may hop to equivalent Co sites orientated along different axes. If the hopping rate is slow compared with the lifetime of the Mössbauer state ($\sim 10^{-7}$ s.) the Fe atom will feel the asymmetric charge distribution calculated. However, if the rate is fast, a more delocalised charge distribution will be apparent, leading to lower quadrupole splittings. This effect may become important at high temperatures. Other arrangements are possible for trapped holes associated with the 4:1 cluster in addition to those considered here. We have chosen only the most symmetrical case. However, the relaxed energy splittings are similar in all the cases studied and other clusters are unlikely to differ greatly. When calculating the electronic contribution to the quadrupole splitting important in Fe^{2+}, (equation 6), the influence of the lattice potential on the electronic levels was not considered, and unperturbed ionic wavefunctions were assumed. In Fe^{2+} the electronic term is an order of magnitude larger than any direct lattice contribution and the second-order effect of the lattice through distortion of the electronic states should be smaller still. Finally, we have not considered the influence of extended defects, such as dislocations which may be introduced in the sample during the quenching process used in preparing the source. Although dislocations cannot contribute to an electric-field gradient, their electric fields can cause inhomogeneous broadening of the resonance line (Stoneham 1969).

The results obtained in these calculations are given in table 4. In each case we give the principal components of the electric-field gradient and the line splitting that should be observed. Also shown are the field gradients calculated assuming the perfect lattice positions. These differ greatly from the results obtained from the relaxed geometry. If we consider the single vacancy defects shown in figure 1, both the V^{2-} and V^{-} centres have identical field gradients (due to the single vacancy) in the perfect lattice. After

Table 4. Electric-field gradients and Mössbauer line splittings for Fe^{2+} and Fe^{3+} in defect configurations in cobalt oxide

Defect centre	Perfect lattice field gradients V_{xx}, V_{yy}, V_{zz} ($Å^{-3}$)	Relaxed lattice field gradients V_{xx}, V_{yy}, V_{zz} ($Å^{-3}$)	Asymmetry parameter η	Line splitting (eV)
V^{2-} (Fe^{2+})	−0·0732	−0·0217	0·4809	$19{\cdot}16 \times 10^{-8}$
	−0·0732	−0·0619		
	0·1463	0·0836		
V^{-} (Fe^{3+})	−0·0732	−0·1149	0·4029	$5{\cdot}46 \times 10^{-8}$
	−0·0732	−0·2699		
	0·1463	0·3847		
V^{0}(Fe^{3+})	−0·0549	−0·1194	0·2666	$4{\cdot}54 \times 10^{-8}$
	−0·0549	−0·2062		
	0·1098	0·3256		
4:1 (Fe^{3+}, tet)	0·0660	−0·1529	0·0	$4{\cdot}22 \times 10^{-8}$
	0·0660	−0·1529		
	−0·1320	0·3059		
4:1 (Fe^{3+}, oct)	0·0337	−0·0265	0·8038	$4{\cdot}12 \times 10^{-8}$
	0·1067	−0·2437		
	−0·1404	0·2702		
4:1 (Fe^{2+}, oct)	0·0257	−0·0090	0·8336	$20{\cdot}86 \times 10^{-8}$
	0·1215	0·0992		
	−0·1471	0·1082		
Spinel (Fe^{2+}, tet)	0·0	—	0·0	$17{\cdot}3 \times 10^{-8}$
	0·0	—		
	0·0	—		
Spinel (Fe^{3+}, oct)	−0·0195	—	0·0	$0{\cdot}54 \times 10^{-8}$
	−0·0195	—		
	0·0390	—		

relaxation, however, the V^{2-} centre has a reduced field gradient ($\sim 57\%$) whereas the V^{-} centre has a greatly enhanced gradient ($\sim 300\%$ of the former value). In addition, in both cases the symmetry of the field gradient is reduced so that $V_{xx} \neq V_{yy}$. Where the unrelaxed field gradient has a symmetry greater than the point group of the defect, relaxation will, in general, introduce asymmetry (see V^{0}(Fe^{3+}) and 4:1 (Fe^{3+}, tet)). Results are also shown for the various sites associated with the 4:1 cluster and similar discrepancies between unrelaxed and relaxed field gradients are observed. The line splittings given in table 4 are calculated from equation (6) and include the electronic term. This dominates the quadrupole splittings for the Fe^{2+} ions which are up to an order of magnitude larger than those for Fe^{3+}. The spinel phase of Co_3O_4 has a normal spinel structure with Co^{2+} in tetrahedral sites with no lattice electric-field gradient and Co^{3+} in distorted octahedral sites. However, the field gradient due to the lattice

at these octahedral sites is very small compared with defect gradients. It leads to a line splitting that is an order of magnitude less than that due to vacancies in CoO, and is therefore unlikely to be confused with them. The natural width of the Fe line is $4{\cdot}7 \times 10^{-9}$ eV and so the splitting due to the spinel structure may not be observable, although the splitting or broadening due to the defects (minimum value = $1{\cdot}98 \times 10^{-8}$) is experimentally detectable.

There is little detailed experimental data on quadrupole splittings of Fe lines in CoO and generally only the linewidth is given and not the calculated quadrupole splitting using a Lorentzian approximation. For example, Sond and Mullen (1976) report a width of $\sim 0{\cdot}7$ mm s^{-1}, for the Fe^{3+} line at room temperature. If this is due to unresolved quadrupole splitting, it gives a value of $\sim 4{\cdot}0 \times 10^{-8}$ eV in good agreement with the splitting caused by defects. Table 5 shows splittings of Fe lines observed in

Table 5. Quadrupole line splittings observed in a variety of crystals

Crystal	$\Delta E(Fe^{2+})$ (eV)	$\Delta E(Fe^{3+})$ (eV)
$CoCl_2.6H_2O$[a]	$10{\cdot}8 \times 10^{-8}$	$5{\cdot}7 \times 10^{-8}$
$Co(NH_4SO_4)_2.6H_2O$[a]	$12{\cdot}9 \times 10^{-8}$	$4{\cdot}8 \times 10^{-8}$
$FeCl_2.4H_2O$[b]	$14{\cdot}9 \times 10^{-8}$	—
$FeSO_4.7H_2O$[b]	$17{\cdot}3 \times 10^{-8}$	
$Fe_{1-x}O$[c]		$2{\cdot}4$–$4{\cdot}4 \times 10^{-8}$
Fe_2O_3[d]		$1{\cdot}2 \times 10^{-8}$
CoO[e]		$\sim 4{\cdot}0 \times 10^{-8}$

[a] Ingalls and De Pascuali 1965
[d] De Benedetti *et al* 1961
[c] Greenwood and Howe 1972
[d] Kistner and Sunyar 1960
[e] Song and Mullen 1976 (linewidths only)

other materials for comparison. In all cases the quadrupole effect in Fe^{2+} is much greater because of the electronic term and, although it can be smaller than the values calculated here, there is evidence that this splitting decreases with temperature (De Benedetti *et al* 1961). Our calculations are for a static lattice and thus refer to absolute zero temperature. The splittings of the Fe^{3+} lines are close to those predicted for the CoO case for all materials except Fe_2O_3, where the linewidth is narrower. Apart from the CoO results, the Fe^{3+} splittings in $Fe_{1-x}O$ are of greatest interest since this non-stoichiometric crystal has the same defect structure as CoO (Catlow *et al* 1977a). Here the energy splitting observed is in close agreement with our calculations.

The main conclusions from this study can be summarised as follows. The higher-charge states of iron (Fe^{3+}) can be produced from the decay of Co^{3+} which is present in CoO and stabilised by cation vacancies. The line splitting observed as a broadening of the Fe^{3+} line is compatible with the field gradients that would be produced by the vacancy clusters. The field gradients produce line splittings which are large compared with the natural linewidth and are thus experimentally observable. The splittings of the Fe^{2+} line are naturally much larger because of the electronic term but the various clusters produce splittings for the Fe^{3+} line that are distinguishable in principle. Finally, we have shown that it is vital to use correctly relaxed lattice geometries for the defect

configuration when calculating the quadrupole interaction. The resulting field gradients differ substantially from those obtained using the unrelaxed geometries: perfect lattice calculations are therefore totally inadequate.

References

Catlow C R A, Fender, B E F and Muxworth D G 1977a *J. Physique* C7 67
Catlow C R A, Mackrodt W C, Norgett M J and Stoneham A M 1977b *Phil. Mag.* **35** 177
De Benedetti S, Lang G and Ingalls R 1961 *Phys. Rev. Lett.* **6** 60
De Wette F W 1961 *Phys. Rev.* **123** 103
Dick B G and Overhauser A W 1958 *Phys. Rev.* **112** 90
Freeman A J and Watson R E 1965 *Hyperfine Interactions in Magnetic Materials* in *Treatise on Magnetism* vol IIA ed G T Suhl and H Rado (New York: Academic Press)
Greenwood N N and Howe A T 1972 *J. Chem. Soc. Dalton* 110
Ingalls R 1964 *Phys. Rev.* A **133** 787
Ingalls R and De Pascuali G 1965 *Phys. Lett.* **15** 262
Kistner O C and Sunyar A W 1960 *Phys. Rev. Lett.* **4** 412
Leon V and Negrete P 1970 *Solid St. Commun.* **8** 740
Lidiard A B and Norgett M J 1972 in *Computational Solid State Physics* ed F Herman, N W Dalton and T R Koehler (New York: Plenum Press)
Mott N F and Littleton M J 1938 *Trans. Faraday Soc.* **34** 485
Mullen J G and Ok H N 1966 *Phys. Rev. Lett.* **17** 287
Norgett M J 1974 *UKAEA Report AERE* R 7650
Norgett M J, Stoneham A M and Pathak A P 1977 *J. Phys. C: Solid St. Phys.* **10** 555
Ok H N and Mullen J G 1968 *Phys. Rev.* **168** 550
Schroeer D and Triftshäusen W 1968 *Phys. Rev. Lett.* **20** 1242
Sen K D and Narasimhan P T 1976 *Phys. Rev.* A**14** 539
Sharma R R 1971 *Phys. Rev. Lett.* **26** 563
Sond C and Mullen J G 1976 *Phys. Rev.* B**14** 2761
Stoneham A M 1969 *Rev. Mod. Phys.* **41** 82
Tejada J and Fontcuberta J 1978 Univ. de Barcelona Preprint
Triftshäuser W and Craig P P 1966 *Phys. Rev. Lett.* **16** 1161
Wertheim G K 1961 *Phys. Rev.* **124** 764